Preliminary analysis of ground-to-flight mechanical tolerances of the Ariel mission telescope

Paolo Chioetto, Andrea Tozzi, Anna Brucalassi, Debora Ferruzzi, Andrew Caldwell, et al.

Published version information:

Citation: P Chioetto et al. Preliminary analysis of ground-to-flight mechanical tolerances of the Ariel mission telescope. Proc SPIE 12180 (2022): 121804R. Is in proceedings of: Space Telescopes and Instrumentation 2022: Optical, Infrared, and Millimeter Wave, Montréal, Québec, Canada, 17-23 Jul 2022.

DOI: 10.1117/12.2628900

Preliminary analysis of ground-to-flight mechanical tolerances of the Ariel mission telescope

Paolo Chioetto, Andrea Tozzi, Anna Brucalassi, Debora Ferruzzi, Andrew Caldwell, et al.

Paolo Chioetto, Andrea Tozzi, Anna Brucalassi, Debora Ferruzzi, Andrew Caldwell, Martin Caldwell, Fausto Cortecchia, Emiliano Diolaiti, Paul Eccleston, Elisa Guerriero, Matteo Lombini, Giuseppe Malaguti, Giuseppina Micela, Emanuele Pace, Enzo Pascale, Raffaele Piazzolla, Giampaolo Preti, Mario Salatti, Giovanna Tinetti, Elisabetta Tommasi, Paola Zuppella, "Preliminary analysis of ground-to-flight mechanical tolerances of the Ariel mission telescope," Proc. SPIE 12180, Space Telescopes and Instrumentation 2022: Optical, Infrared, and Millimeter Wave, 121804R (27 August 2022); doi: 10.1117/12.2628900

Event: SPIE Astronomical Telescopes + Instrumentation, 2022, Montréal, Québec, Canada

Preliminary analysis of ground-to-flight mechanical tolerances of the Ariel mission telescope

Paolo Chioetto*[a,b,c], Andrea Tozzi[d], Anna Brucalassi[d], Debora Ferruzzi[d], Andrew Caldwell[f], Martin Caldwell[f], Fausto Cortecchia[e], Emiliano Diolaiti[e], Paul Eccleston[f], Elisa Guerriero[m], Matteo Lombini[e], Giuseppe Malaguti[e], Giuseppina Micela[g], Emanuele Pace[h], Enzo Pascale[i], Raffaele Piazzolla[k], Giampaolo Preti[h], Mario Salatti[k], Giovanna Tinetti[l], Elisabetta Tommasi[k], and Paola Zuppella[c]

[a]CNR-Istituto di Fotonica e Nanotecnologie di Padova, Via Trasea 7, 35131 Padova, Italy
[b]Centro di Ateneo di Studi e Attività Spaziali "Giuseppe Colombo"- CISAS, Via Venezia 15, 35131 Padova, Italy
[c]INAF-Osservatorio Astronomico di Padova, Vicolo dell'Osservatorio 5, 35122 Padova, Italy
[d]INAF-Osservatorio Astrofisico di Arcetri, Largo E. Fermi 5, 50125 Firenze, Italy
[e]INAF-Osservatorio di Astrofisica e Scienza dello spazio di Bologna, Via Piero Gobetti 93/3, 40129 Bologna, Italy
[f]RAL Space, STFC Rutherford Appleton Laboratory, Didcot, Oxon, OX11 0QX, UK
[g]INAF-Osservatorio Astronomico di Palermo, Piazza del Parlamento 1, 90134 Palermo, Italy
[h]Dipartimento di Fisica ed Astronomia-Università degli Studi di Firenze, Largo E. Fermi 2, 50125 Firenze, Italy
[i]Dipartimento di Fisica, La Sapienza Università di Roma, Piazzale Aldo Moro 2, 00185 Roma, Italy
[j]INAF-IAPS,Via del Fosso del Cavaliere 100, I-00133 Rome, Italy
[k]ASI, Agenzia Spaziale Italiana, Via del Politecnico snc, Roma, Italy
[l]Department of Physics and Astronomy, University College London, Gower Street, London WC1E 6BT, UK
[m]Dipartimento di Fisica e Chimica-Università degli Studi di Palermo, Via Archirafi 36, 90128 Palermo, Italy

ABSTRACT

Ariel (Atmospheric Remote-Sensing Infrared Exoplanet Large Survey) is the adopted M4 mission of ESA "Cosmic Vision" program. Its purpose is to conduct a survey of the atmospheres of known exoplanets through transit spectroscopy. Launch is scheduled for 2029. Ariel scientific payload consists of an off-axis, unobscured Cassegrain telescope feeding a set of photometers and spectrometers in the waveband between 0.5 and 7.8 µm, and operating at cryogenic temperatures.

The Ariel Telescope consists of a primary parabolic mirror with an elliptical aperture of 1.1 m of major axis, followed by a hyperbolic secondary, a parabolic recollimating tertiary and a flat folding mirror directing the output beam parallel to the optical bench. The secondary mirror is mounted on a roto-translating stage for adjustments during the mission.

Proper operation of the instruments prescribes a set of tolerances on the position and orientation of the telescope output beam: this needs to be verified against possible telescope misalignments as part of the ongoing Structural, Thermal, Optical and Performance Analysis.

A specific part of this analysis concerns the mechanical misalignments, in terms of rigid body movements of the mirrors, that may arise after ground alignment, and how they can be compensated in flight. The purpose is

*paolo.chioetto@pd.ifn.cnr.it

Space Telescopes and Instrumentation 2022: Optical, Infrared, and Millimeter Wave, edited by Laura E. Coyle, Shuji Matsuura, Marshall D. Perrin, Proc. of SPIE Vol. 12180, 121804R · © 2022 SPIE · 0277-786X · doi: 10.1117/12.2628900

to derive the mechanical constraints that can be used for the design of the opto-mechanical mounting systems of the mirrors.

This paper describes the methodology and preliminary results of this analysis, and discusses future steps.

Keywords: space telescope, Ariel mission, tolerancing, Cassegrain, aluminum mirror, STOP Analysis

1. INTRODUCTION

Ariel is the M4 mission of ESA "Cosmic Vision" program, with the scientific purpose of carrying out a survey of the atmospheres of a large sample of known exoplanets. Officially adopted in 2020, Ariel is scheduled to launch in 2029.[1] The payload consists of a set of spectrometers and photometers operating in the waveband 0.5 µm to 7.8 µm, fed by an afocal, unobscured Cassegrain-type telescope.[2]

The Cassegrain is designed off-axis, with a large elliptical entrance pupil of 0.6 m^2 of area, followed by a tertiary recollimating mirror and a fourth folding mirror that bends the light beam towards the optical bench. The global optical coordinate reference (OPT) for the telescope has its center at the vertex of the parent parabola of M1, and the axes oriented as in Fig. 1. The secondary mirror is mounted on a mechanism (M2M) permitting regulation of tip/tilt and shift along the optical axis (focus) for fine adjustments during flight. The telescope has diffraction limited optical performance at the wavelength of 3 µm and on a 30″ Field of View (FoV). Telescope and instruments will operate at a temperature below 50 K.

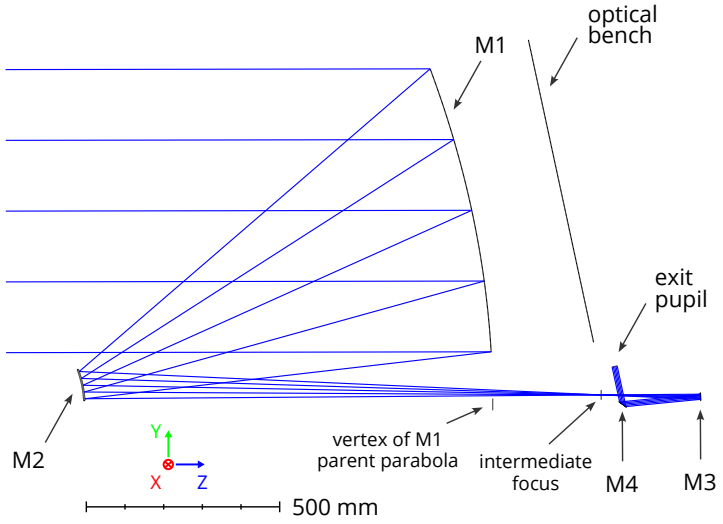

Figure 1. Ariel Telescope optical design.

The baseline material for the telescope mirrors and supporting structures, chosen on the criteria of athermalization, ease of construction and cost, is aluminum alloy 6061-T651. Aluminum has a relatively high coefficient of thermal expansion compared with other mirrors construction materials such as glass-ceramics, and a low stiffness, so a detailed thermal and termo-mechanical analysis is required to determine the extent of deformations induced at the operating temperature by thermal gradients and mechanical stresses, and their effects on optical performance. The analysis, known with the acronym STOP from the initials of Structural, Thermal, Optical Performance Analysis, consists of a series of cases with specific boundary conditions set in terms of temperature maps and mechanical loads.

The analysis presented here is complementary to the STOP Analysis, and is concerned with another possible source of optical performance degradation: the effect of rigid body motions of the mirrors with respect to their nominal position (misalignments), caused for example by dynamic loads (accelerations and vibrations) during launch. For this case, as opposed to thermo-elastic deformation, it is not always feasible to determine analytically

the direction and extent of the motions, so a statistical approach is required. This is especially true for the analysis presented here since, at the current level of development, a detailed mechanical design of the mountings of the mirrors is not yet finalized.

The purpose of the analysis is twofold: the first, given a set of requirements on the optical performance and the position and orientation of the telescope collimated output beam, is to determine the maximum range of misalignments that can still be tolerated with respect to the requirements and the second, reversing the analysis, is to calculate the maximum effect on performance given the extent of the misalignments.

Optical performance is evaluated in terms of Enclosed Energy (EE) within a specific area of the Point Spread Function (PSF), at the exit pupil of the telescope. More specifically, since the footprint of the exit pupil is elliptical, as it is the image of the elliptical aperture of the primary mirror, what is actually computed is the percentage of energy within an ellipse. The size of the EE ellipse has been determined through simulation from the scientific requirements of the mission.

Position and orientation of the exit beams, on the other hand, are measured in reference to a plane that is orthogonal to the beam, and placed at the exit pupil of the telescope. The position is calculated at the intersection of the chief ray (the ray passing through the center of the entrance pupil) with the plane, while the orientation as the exit angle of the chief ray.

2. SIMULATION SETUP

The starting point for the analysis presented here is the nominal telescope design at the operating temperature of 50 K.

Aim of the analysis is to determine the maximum misalignments that are still recoverable using the two compensation mechanisms available in flight: the secondary mirror M2, and a tilt of the line of sight (LoS) of the entire telescope.

The analysis is carried out with the aid of the optical simulation software Zemax OpticStudio©, and routines written by the author in Python. The amount of compensation is calculated through the optimization functionality of OpticStudio, employing a Merit Function (MF) based on Encircled Energy and maximum allowed displacements of the Telescope exit pupil (more on this in Section 2.3).

The steps used in the analysis are:

1. an initial inverse sensitivity analysis to determine the range of admissible misalignments for each element taken individually, based on the acceptable range of performance parameters (acceptance criteria);
2. a Monte Carlo simulation on the ranges identified in Step 1 to evaluate statistically the combined effect of multiple misalignments.

Tilts and shifts of each mirror are relative to the local reference frame as defined by the simulation software, and a center of rotation (CoR) (Fig. 2).

For M1, M3 and M4 the CoR is arbitrarily positioned at the center of the optical surface, since the details of the mounting mechanism are still being finalized. For M2 the CoR of the M2M mechanism is known, so it is used also as center of rotation for the misalignments.

2.1 Acceptance Criteria

The set of acceptance criteria, derived from telescope requirements, are the percentage of Enclosed Energy that is lost with respect to the nominal design and the exit beam shift and tilt at the nominal exit pupil. They are reported in Table 1, together with their knowledge error.

The baseline requirement for Enclosed Energy at the wavelength of 0.55 µm is given for an ellipse with semi-axes 41″ and 27″, and imposes that at least 83.8% of the energy of the PSF at the telescope exit pupil be within the ellipse, for all fields within the telescope FoV.

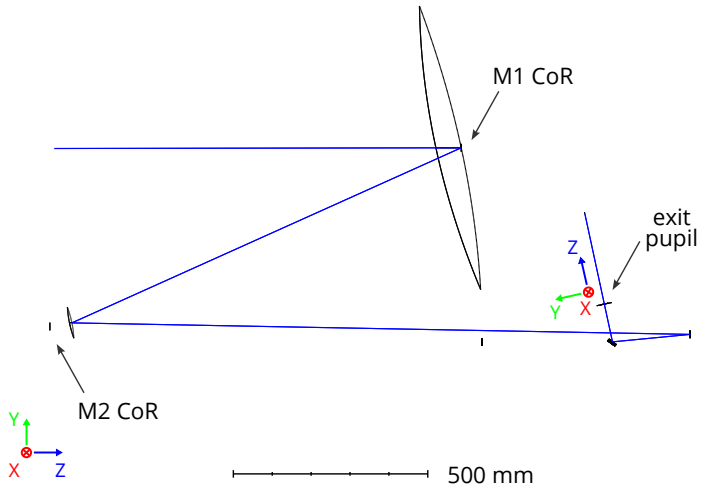

Figure 2. Diagram of the optical design used in the simulations, showing the chief ray (blue), global (left) and local (right, at the EXP surface) axes orientations, and Centers of Rotation (CoR) for M1 and M2.

Table 1. Acceptable performance range for ground-to-flight misalignment errors. Corresponding TA requirement are also indicated.

Parameter	Allowed Range	Knowledge Error
Lost EE	$\leq 5\,\%$	–
Beam Tilt x/y	$\pm 45''$	$\pm 15''$
Beam Shift x/y	$\pm 60\,\mu m$	$\pm 20\,\mu m$

If we consider the nominal telescope design, that is close to diffraction limit, the energy enclosed in the such ellipse is at least 96%, so the margin is 12.2%. The figure of 5%, used for this simulation, is an arbitrary allocation of this margin.

This is so because the ellipse from the requirement for radial Encircled Energy at 0.55 µm, as given above, is larger than the "diffraction limited" ellipse that has axes of $10.4''$ and $6.9''$, according to the approximated formula for the first minimum of the Airy disk with $\lambda = 0.55\,\mu m$:

$$\theta = 1.22\frac{\lambda}{D},$$

and with D equal to the major and minor axes of the telescope entrance pupil (730 and 1100 mm), and taking into consideration the telescope angular magnification of 55.

Admissible tilts and shifts of the exit beam have instead been derived from alignment requirements of the instruments downstream from the telescope.

2.2 Compensators

At each step of the inverse sensitivity analysis and the Monte Carlo simulation, the perturbed system is re-optimized using the compensators within the nominal ranges specified in Table 2.

The Line of Sight (LoS) compensation is a rigid body rotation of the entire telescope, resulting in fact in a re-pointing to an off-axis field. It is easy to see how this compensation results in a tilt of the exit beam with a scale factor equal to the magnification of the telescope.

M2 compensations are applied wrt. the M2M movement origin, which is located behind the M2 mirror vertex, at a point with the following coordinates: +40.1 mm in the y_{OPT} direction from M2 vertex and -61.8 mm in the z_{OPT} direction from M2 vertex.

Table 2. Compensators rages for the ground-to-flight case.

Compensator	Allowed Range
M2 Tip/Tilt	±0.115° (414″)
M2 z-axis translation	±350 µm
Line of Sight rotation (x/y axes)	–

2.3 Optimization Function

OpticStudio local optimization functionality[3,4] utilizes a proprietary version of the damped least squares algorithm to minimize a target function, known as Merit Function (MF), by varying a set of parameters. In our case the parameters correspond to the set of compensators specified in Section 2.2.

The MF is specified using various operands, and for both the inverse sensitivity analysis and the Monte Carlo simulation, consists of the following terms, all contributing equally.

1. An approximation of the lost Enclosed Energy (1 - EE) of the PSF at the exit pupil, taking the maximum value calculated for eight radial fields at the edge of the 30″ field of view of the telescope. The wavelength of 0.55 µm is considered.
2. The direction cosines of the chief ray at the exit pupil ("REAA" and "REAB" operands). These values are derived from the angle at which the incoming beam exits the surface that materializes the Exit Pupil.
3. The local x and y coordinates of the intersection of the chief ray for the on-axis field at the Exit Pupil ("REAX" and "REAY").

OpticStudio does not provide a way to calculate the fraction of energy enclosed in an elliptical aperture in the PSF. For this reason, an approximation is made by calculating the energy enclosed in the two circles inscribing and circumscribing the ellipse, and averaging the two, as illustrated in Figure 3 for a sample aberrated PSF. The approximation was found to be reasonably good for the intended purposes.[5]

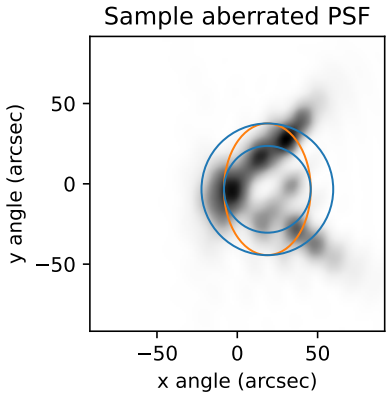

Figure 3. Sample aberrated PSF illustrating the approximated calculation of the Enclosed Energy on the circles inscribing and circumscribing an elliptic aperture.

The direction cosines of point 2 above ("REAA" and "REAB") are the cosines of the angles that the chief ray vector forms with the x, y axes, so the relation with the beam angle is:

$$\theta_{\{x/y\}} = \pi/2 - \arccos(\{\text{REAA/REAB}\})$$

Each term is evaluated using "greater than" or "less than" operands ("OPGT" and "OPLT") against the mandated ranges of variation, so its contribution to the MF goes to zero as soon as the corresponding requirement is satisfied, and therefore the MF equals zero when all requirements are satisfied.

Table 3 summarizes the operands used.

The operands evaluating the position and orientation of the exit pupil must be employed on the surface that is located at the actual position of the exit pupil along the local z axis, in the perturbed telescope design, which may move slightly, changing the calculation of the x and y intersection coordinates.

For this reason, the surface materializing the exit pupil in the nominal design is preceded by an auxiliary surface of variable thickness, and an additional optimization operand, "EXPP", is employed to make sure that the surface marked as "exit pupil" is indeed located at the exit pupil of the telescope, even in the perturbed design (in the paraxial approximation).

The Merit Function presented above is very computationally intensive because of the "DENF" operands, that require calculation of the PSF to determine the radius of encircled energy. For this reason, the final optimization of each configuration is preceded by a "pre-optimization" step using a less intensive Merit Function based on the root mean squared (RMS) size of the Spot Radius. This step can be seen as a way to bring the perturbed telescope close to the optimal compensation very quickly, before performing the last optimization step.

Since the final evaluation of the optimized case is performed on the proper merit function using DENF operands, the procedure is equivalent in terms of results.

Please also note that no global optimization algorithm has been applied in the procedure, so it is possible that some cases result non compliant when the MF does not converge to zero because it is stuck in a local minimum outside the acceptance criteria range. Some of the non compliant cases where therefore checked manually, but were rarely found to be false negatives.

Table 3. Operands used in the OpticStudio optimization Merit Function.

	Operand Used	Explanation
Lost EE	DENF	Average of EE on circles inscribed and circumscribed on elliptical aperture
EXP Tilt x	REAA on EXP	Chief Ray angle (deg) with local x axis (parallel to global x)
EXP Tilt y	REAB on EXP	Chief Ray angle (deg) with local y axis (orthogonal to OB)
EXP Shift x	REAX on EXP	Chief Ray x shift (mm)
EXP Shift y	REAY on EXP	Chief Ray y shift (mm)
EXP Position	EXPP	Paraxial exit pupil position

3. RESULTS

The simulation setup described in the previous sections was applied to two scenarios, identified by the set of acceptance criteria utilized.

Scenario 1 Nominal acceptance criteria defined in Paragraph 2.1. The analysis consists of an inverse sensitivity to determine the maximum perturbation ranges, a Monte Carlo simulation with the maximum perturbation ranges and finally a Monte Carlo with a set of perturbations with reduced ranges derived from industry expertise;

Scenario 2 Inverse sensitivity analysis with a relaxed set of acceptance criteria.

3.1 Nominal Acceptance Criteria Scenario

3.1.1 Inverse Sensitivity Analysis

The goal of the inverse sensitivity analysis procedure is to determine the maximum range of perturbations that, applied one at a time, can still be compensated to achieve a telescope configuration that is compliant with requirements.

The procedure consists of the following steps, applied to each parameter:

1. start from the unperturbed optical design;
2. perturb a single parameter and re-optimize the optical model using compensators, until the MF can converge to zero, meaning that the design has been compensated within requirement;
3. increase the magnitude of the perturbation until a value is reached beyond which the design can no longer be optimized, or the limits of the compensators are reached (this is done independently for the positive and negative extremes of the range).

In Table 4 we report the maximum and minimum values of the tolerance operands, and the compensation applied. The limits imposed on operands "REAA" and "REAB" are 2.182×10^{-4}, calculated with the following formula:

$$\cos\left(\frac{\pi}{2} - \theta_{\{x/y\}}\right)$$

where $\theta_{x/y}$ are the components in x and y in radians of the chief ray angle wrt. the surface normal (equal to the $45''$ range limit of Table 1).

3.1.2 Monte Carlo Simulation with maximum perturbation ranges

A Monte Carlo simulation was then ran to consider the effect of all perturbations derived in the previous section, applied simultaneously. For each Monte Carlo case, all the parameters are assigned a random value from a uniform probability distribution in the perturbation interval (Table 4).

The goal of the simulation is to determine the percentage of compliant cases, i.e. cases that can be optimized to be within telescope requirements using the two steps optimization merit function described in paragraph 2.3.

This simulation was performed in order to get a sense of how sensitive the telescope design is in terms of the combination of more than one displacements, and in fact only 17 cases resulted viable out of the total run of 100.

3.1.3 Monte Carlo Simulation with reduced perturbation ranges

The Monte Carlo simulation was then repeated using a set of reduced displacement ranges of $\pm 10\,\mu m$ for linear shifts and $\pm 10''$ for rotations.

The new set was devised based on feedback from the telescope prime contractor that the displacements can be greatly reduced from the ranges determined from the inverse sensitivity analysis, upon considerations that the primary mirror can be hold in position by pins, and that no specific challenges are foreseen for the mounting of the smaller mirrors.

Before proceeding with the actual Monte Carlo, the boundary cases of each reduced range was optimized separately, to determine the effect on the system. Results, presented in Table 5, show how each case can be compensated. Results are in line with those of Table 4, showing that smaller perturbations require smaller adjustments of the same compensators.

Then the Monte Carlo analysis was performed, assigning random values from uniform probability distributions in the perturbation intervals to all parameters.

With this new reduced set of ranges, 98% of the cases are recoverable with compensation (up from 17% in the previous case).

Table 6 shows the statistics of the results of the simulation, while the statistics on the values attained by the compensators after the optimizations are shown in Table 7. Note that in this case compensation does not require using the entire M2M range of motion, but 9% of the range for the shift along the optical axis and 63% of the range for the the tilts.

Table 4. Maximum and minimum values for the tolerance operands for the nominal acceptance scenario. Cells highlighted in red color are values at the extreme of the acceptable range, while cells in yellow are close to the limit.

			Compensators				
Mirror	Parameter	Range	M2 Focus (mm)	M2 Tilt-x (deg)	M2 Tilt-y (deg)	LoS Tilt-x (deg)	LoS Tilt-y (deg)
M1	TILT X	0.0051	0.037	0.109	0.000	0.006	0.000
	(range in deg)	-0.0052	-0.036	-0.109	0.000	-0.005	0.000
	TILT Y	0.0053	0.000	-0.001	0.115	0.000	0.006
	(range in deg)	-0.0053	0.000	-0.001	-0.114	0.000	-0.006
	DEC X	0.1030	-0.002	-0.006	-0.115	-0.001	-0.011
	(range in mm)	-0.1030	0.000	-0.002	0.115	0.000	0.011
	DEC Y	0.0980	0.081	0.109	0.000	0.011	0.000
	(range in mm)	-0.1010	-0.082	-0.109	0.000	-0.011	0.000
	MOVE Z	0.3610	0.350	-0.012	0.000	-0.002	0.000
	(range in mm)	-0.3630	-0.350	0.021	0.000	0.003	0.000
M2	DEC X	0.1030	0.000	-0.003	0.115	-0.001	0.011
	(range in mm)	-0.1030	0.000	-0.003	-0.115	0.000	-0.011
	DEC Y	0.1000	-0.086	-0.115	0.000	-0.012	0.000
	(range in mm)	-0.1030	0.086	0.115	0.001	0.011	0.000
M3	TILT X	0.0069	0.009	0.022	0.000	0.004	0.000
	(range in deg)	-0.0069	-0.010	-0.022	0.000	-0.003	0.000
	TILT Y	0.0066	0.000	0.001	0.018	0.000	0.002
	(range in deg)	-0.0066	0.000	0.000	-0.018	0.000	-0.002
	DEC X	0.0590	0.000	0.000	-0.018	0.000	-0.003
	(range in mm)	-0.0580	-0.001	-0.003	0.018	0.000	0.003
	DEC Y	0.0610	0.008	0.021	0.007	0.003	0.001
	(range in mm)	-0.0610	-0.010	-0.021	-0.001	-0.003	0.000
	MOVE Z	0.7600	-0.001	-0.019	0.000	-0.003	0.000
	(range in mm)	-0.7600	0.001	0.019	0.000	0.003	0.000
M4	TILT X	0.0180	-0.004	-0.005	0.001	-0.001	0.000
	(range in deg)	-0.0200	0.008	0.017	0.000	0.003	0.000
	TILT Y	0.0290	0.000	-0.003	-0.014	0.000	-0.002
	(range in deg)	-0.0290	0.000	0.000	0.014	0.000	0.002
	MOVE Z	0.0480	-0.009	-0.023	0.000	-0.003	0.000
	(range in mm)	-0.0480	0.008	0.021	-0.001	0.003	0.000

3.2 Relaxed Acceptance Criteria Scenario

This paragraph presents an additional simulation scenario with an arbitrary set of relaxed requirements on exit pupil position and orientation and encircled energy (Table 8). The purpose is to assess dependency of the tolerances on the requirements.

The analysis was performed on M1 only, as results for this mirror already show that relaxing the requirements does not lead to a significant improvement in the range of admissible perturbations.

The analysis seems to point to a strong dependence of the results to the limits in the range of motion of the M2M compensator.

Table 9 and Table 10 present the results of the inverse sensitivity analysis on the Relaxed Requirements scenario and the comparison with the Base Scenario, respectively.

Table 5. Configuration of compensators that optimize each of the extremes of the reduced perturbation ranges of $\pm 10\,\mu m$ for linear shifts and $\pm 10''$ for rotations. M3 and M4 are not shown since their perturbations do not require reoptimization to comply with requirements.

			Compensators				
Mirror	Parameter	Range	M2 Focus (mm)	M2 Tilt-x (deg)	M2 Tilt-y (deg)	LoS Tilt-x (deg)	LoS Tilt-y (deg)
M1	TILT X	0.0028	0.025	0.070	0.000	0.004	0.000
	(range in deg)	-0.0028	-0.025	-0.069	0.000	-0.005	0.000
	TILT Y	0.0028	0.000	0.000	0.069	0.000	0.004
	(range in deg)	-0.0028	0.000	0.000	-0.069	0.000	-0.004
	DEC X	0.0100	0.000	0.000	-0.002	0.000	0.000
	(range in mm)	-0.0100	0.000	0.000	-0.001	0.000	0.000
	DEC Y	0.0100	0.001	0.001	0.002	0.000	0.000
	(range in mm)	-0.0100	-0.001	-0.003	0.000	0.000	0.000
	MOVE Z	0.0100	0.010	0.000	0.000	0.000	0.000
	(range in mm)	-0.0100	-0.010	0.000	0.000	0.000	0.000
M2	DEC X	0.0100	0.000	0.000	0.001	0.000	0.000
	(range in mm)	-0.0100	0.000	0.000	-0.001	0.000	0.000
	DEC Y	0.0100	-0.020	-0.020	0.000	0.000	0.000
	(range in mm)	-0.0100	0.010	0.010	0.010	0.000	0.000

Table 6. Statistical description of Monte Carlo results (500 cases) with uniform parameters distribution. Absolute values of parameters are used for the statistics.

	beam shift (mm)		beam tilt (arcsec)		EE lost
	x	y	x	y	
min	0	0	0.1	0.4	4.15%
50%	0.021	0.023	45.0	45.0	4.18%
75%	0.034	0.039	45.0	45.0	4.20%
90%	0.048	0.051	45.0	45.0	4.23%
95%	0.055	0.057	45.0	45.0	4.66%
max	0.061	0.065	45.3	46.4	6.54%

Table 7. Statistics of compensators for the compliant cases from the Monte Carlo run. *EXP shift* is the shift along the optical axis of the paraxial exit pupil position. Tilts are in degrees, shifts in mm.

	M2			LoS		EXP shift
	z shift	x tilt	y tilt	x tilt	y tilt	
min	0.0000	0.0002	0.0000	-0.006	0.0000	0.0000
50%	0.0127	0.0350	0.0372	0.0001	0.0021	0.0070
75%	0.0205	0.0518	0.0523	0.0021	0.0031	0.0118
80%	0.0226	0.0558	0.0550	0.0025	0.0034	0.0131
90%	0.0270	0.0656	0.0647	0.0035	0.0041	0.0161
95%	0.0318	0.0714	0.0719	0.0041	0.0047	0.0186
max	0.0416	0.0816	0.0902	0.0057	0.0065	0.0253

Table 8. Beam position and orientation and Enclosed Energy for the relaxed acceptance criteria scenario.

Parameter	Required range	Relaxed range
Lost EE	≤5 %	≤7 %
Beam Tilt x	±45″	±150″
Beam Tilt y	±45″	±150″
Beam Shift x	±60 µm	±100 µm
Beam Shift y	±60 µm	±100 µm

Table 9. Inverse sensitivity analysis results on the relaxed requirements scenario.

			Compensators				
Mirror	Parameter	Range	M2 Focus (mm)	M2 Tilt-x (deg)	M2 Tilt-y (deg)	LoS Tilt-x (deg)	LoS Tilt-y (deg)
M1	TILT X	0.0058	0.039	0.115	0.003	0.006	0.001
	(range in deg)	-0.0059	-0.039	-0.115	0.001	-0.005	0.001
	TILT Y	0.0058	0.002	0.003	0.115	0.001	0.005
	(range in deg)	-0.0058	0.000	-0.002	-0.115	0.000	-0.005
	DEC X	0.1110	0.000	-0.002	-0.115	0.000	-0.011
	(range in mm)	-0.1110	0.000	-0.002	0.115	-0.001	0.011
	DEC Y	0.1120	0.089	0.115	-0.003	0.011	-0.001
	(range in mm)	-0.1150	-0.089	-0.115	0.000	-0.011	0.000
	MOVE Z	0.3690	0.350	-0.035	-0.002	-0.006	-0.001
	(range in mm)	-0.3690	-0.350	0.035	-0.002	0.006	-0.001

Table 10. Comparison of inverse sensitivity results for the Base and Relaxed Requirements scenarios.

Mirror	Parameter	Base Scenario	Relaxed Scenario
M1	TILT X (deg)	0.0051	0.0058
		-0.0052	-0.0059
	TILT Y (deg)	0.0053	0.0058
		-0.0053	-0.0058
	DEC X (mm)	0.1030	0.1110
		-0.1030	-0.1110
	DEC Y (mm)	0.0980	0.1120
		-0.1010	-0.1150
	MOVE Z (mm)	0.3610	0.3690
		-0.3630	-0.3690

4. CONCLUSIONS AND NEXT STEPS

The analyses presented in this paper serve as a starting point to understand the range of misalignments that are recoverable in flight by the Ariel telescope, in terms of the requirements on alignment and optical performance of the exit beam, and the effects of the range of misalignments that are considered achievable by the manufacturer.

The two inverse sensitivity analyses of Sections 3.1.1 and 3.2 show that the telescope is very sensitive to small misalignments, especially tilts of M1: a tilt of $21''$ around the x or y axis already produces a configuration that cannot be recovered even with the relaxed requirements on the exit pupil position and orientation.

Monte Carlo simulations show that combining all perturbations from the maximum perturbation ranges leads to a large percentage of non-recoverable cases.

Restricting the perturbation ranges to much smaller values that are deemed as realistic by the telescope manufacturing Prime Contractor, leads however to the vast majority of cases to be recoverable with the M2M using at most 63% of the range of motion for tilts (and a much smaller percentage for focus).

These analyses will need to be integrated with the results from STOP Analysis and with the expected margins of the on-ground alignment plan.

ACKNOWLEDGMENTS

This activity has been realized under the the Implementation Agreement n. 2021-5-HH.0 of the Italian Space Agency (ASI) and the National Institute for Astrophysics (INAF) Framework Agreement "Italian Participation to Ariel mission phase B2/C".

REFERENCES

[1] Tinetti, G. et al., "A chemical survey of exoplanets with ARIEL," *Experimental Astronomy* **46**, 135–209 (Nov. 2018).

[2] Da Deppo, V., Middleton, K., Focardi, M., Morgante, G., Claudi, R., Pace, E., and Micela, G., "The optical configuration of the telescope for the ARIEL ESA mission," in [*Space Telescopes and Instrumentation 2018: Optical, Infrared, and Millimeter Wave*], MacEwen, H. A., Lystrup, M., Fazio, G. G., Batalha, N., Tong, E. C., and Siegler, N., eds., 161, SPIE, Austin, United States (Aug. 2018).

[3] Sahin, F. E., "Open-source optimization algorithms for optical design," *Optik* **178**, 1016–1022 (Feb. 2019).

[4] Zemax LLC, "OpticStudio User Manual," (2022).

[5] Diolaiti, E., Brucalassi, A., Chioetto, P., Cortecchia, F., Ferruzzi, D., Guerriero, E., Lombini, M., Pascale, E., and Tozzi, A., "Ariel Payload Consortium Phase B2 Payload Study - Telescope Assembly Zemax OpticStudio® Tools for Statistical Analysis of Optical Tolerances," ARIEL-INAF-PL-TN-015 (2021).